Molecular Basis for the Dynamic Strength of the Integrin $\alpha_4\beta_1$/VCAM-1 Interaction

Xiaohui Zhang,* Susan E. Craig,† Hishani Kirby,‡ Martin J. Humphries,† and Vincent T. Moy*
*Department of Physiology and Biophysics, University of Miami School of Medicine, Miami, Florida, USA; †Wellcome Trust Centre for Cell-Matrix Research, School of Biological Sciences, University of Manchester, Manchester, United Kingdom; and ‡Celltech Group, Slough, United Kingdom

ABSTRACT Intercellular adhesion mediated by integrin $\alpha_4\beta_1$ and vascular cell adhesion molecule-1 (VCAM-1) plays a crucial role in both the rolling and firm attachment of leukocytes onto the vascular endothelium. Essential to the $\alpha_4\beta_1$/VCAM-1 interaction is its mechanical strength that allows the complex to resist the large shear forces imposed by the bloodstream. Herein we employed single-molecule dynamic force spectroscopy to investigate the dynamic strength of the $\alpha_4\beta_1$/VCAM-1 complex. Our force measurements revealed that the dissociation of the $\alpha_4\beta_1$/VCAM-1 complex involves overcoming at least two activation potential barriers: a steep inner barrier and a more elevated outer barrier. The inner barrier grants the complex the tensile strength to withstand large pulling forces (>50 pN) and was attributed to the ionic interaction between the chelated Mg^{2+} ion at the N-terminal A-domain of the β_1 subunit of $\alpha_4\beta_1$ and the carboxyl group of Asp-40 of VCAM-1 through the use of site-directed mutations. In general, additional mutations within the C-D loop of domain 1 of VCAM-1 suppressed both inner and outer barriers of the $\alpha_4\beta_1$/VCAM-1 complex, while a mutation at Asp-143 of domain 2 of VCAM-1 resulted in the suppression of the outer barrier, but not the inner barrier. In contrast, the outer barrier of $\alpha_4\beta_1$/VCAM-1 complex was stabilized by integrin activation. Together, these findings provide a molecular explanation for the functionally relevant kinetic properties of the $\alpha_4\beta_1$/VCAM-1 interaction.

INTRODUCTION

To serve their functions, blood leukocytes must leave systemic circulation and migrate into lymphoid tissues or to the sites of inflammation. This process, termed extravasation, is mediated by the adhesive interactions between molecules present on leukocytes and their counterreceptors expressed on the vascular endothelium (Springer, 1990). Among these interactions, the adhesion complex formed by leukocyte integrin $\alpha_4\beta_1$ (very late antigen-4, VLA-4) and its endothelial ligand vascular cell adhesion molecule-1 (VCAM-1) is essential for the extravasation of many leukocyte subtypes (Kubes, 2002).

Integrin $\alpha_4\beta_1$ is formed by the noncovalent association of the integrin α_4 (molecular mass ~155 kDa) and β_1 (molecular mass ~150 kDa) subunits (Hemler et al., 1987). $\alpha_4\beta_1$ is expressed on most leukocytes, including lymphocytes, mast cells, eosinophils, natural killer cells, and monocytes. $\alpha_4\beta_1$ has two known ligands, VCAM-1 and the extracellular matrix protein, fibronectin. VCAM-1 is expressed on endothelial cells in two alternately spliced forms, a major form consisting of seven Ig-like domains (VCAM-1(7D)) and a minor form, lacking domain 4 (Osborn et al., 1994). VCAM-1(7D) has two homologous binding sites for $\alpha_4\beta_1$. One site has been localized to domains 1 and 2 and the second to domains 4 and 5. The binding of $\alpha_4\beta_1$ to VCAM-1 involves contributions from the N-terminal domains of both α_4 and β_1 subunits of $\alpha_4\beta_1$. The β_1 A-domain contains a metal ion-dependent adhesion site (MIDAS) that has been implicated in VCAM-1 binding (Vonderheide et al., 1994). In addition, repeats 2–4 of the N-terminal seven-bladed β-propeller domain of α_4 have also been shown to be important for VCAM-1 binding. The most crucial interaction in the stabilization of the $\alpha_4\beta_1$/VCAM-1 complex appears to be the electrostatic interaction between Asp-40 of domain 1 (D1) of VCAM-1 and the chelated Mg^{2+} ion of the β_1 A-domain. Besides Asp-40, other residues that are part of the C-D loop (i.e., T37QIDSPLN) of D1 of VCAM-1 have been shown to be important in $\alpha_4\beta_1$ binding (Vonderheide et al., 1994). In addition, recent studies suggested that domain 2 of VCAM-1 is also involved in stabilizing the $\alpha_4\beta_1$/VCAM-1 complex (Newham et al., 1997).

The main purpose of this research is to understand the molecular basis by which the $\alpha_4\beta_1$/VCAM-1 interaction is able to resist a pulling force. Such studies provide important insight into how activated leukocytes are able to remain adherent to the endothelium in the presence of the shear force of the bloodstream. Although the equilibrium binding affinity constant of the $\alpha_4\beta_1$/VCAM-1 complex has been measured by competitive binding assays (Chigaev et al., 2003), these measurements cannot be used to extrapolate the unbinding force of the complex (Moy et al., 1994). To access the mechanical properties of the $\alpha_4\beta_1$/VCAM-1 complex, we have employed the atomic force microscope (AFM) (Binnig et al., 1986; Hörber and Miles, 2003; Radmacher et al., 1992)

Submitted May 10, 2004, and accepted for publication August 24, 2004.

Address reprint requests to Vincent T. Moy, Dept. of Physiology and Biophysics, University of Miami School of Medicine, 1600 N.W. 10th Ave., Miami, FL 33136. Tel.: 305-243-3201; Fax: 305-243-5931; E-mail: vmoy@newssun.med.miami.edu.

Xiaohui Zhang's present address is CBR Institute for Biomedical Research, Harvard Medical School, Boston, MA 02115.

0006-3495/04/11/3470/09 $2.00

doi: 10.1529/biophysj.104.045690

to measure the loading rate dependence of complex unbinding (i.e., its dynamic force spectrum (DFS)) (Merkel et al., 1999) and to characterize the dissociation potential of the complex. Subsequent mutagenesis experiments permitted us to correlate molecular determinants in VCAM-1 to features in the dissociation potential of the complex.

METHODS

Reagents

$\alpha_4\beta_1$-Fc was generated and purified according to Stephens et al. (2000). To avoid the complicity of two different binding sites on VCAM-1(7D) in our experiments, we used a recombinant truncated form of VCAM-1 containing only the first two domains, VCAM-1(2D)Fc (Newham et al., 1997). VCAM-1(2D)Fc mutants were generated by the method of Kunkel et al. (1987) and have been described earlier (Newham et al., 1997). Purified VCAM-1(2D)Fc was isolated from COS-1 cells transfected with the pIg-VCAM cDNA. Human function-blocking antibody AF809 (anti-VCAM-1) was purchased from R & D Systems (Minneapolis, MN). All other reagents were from Sigma (St. Louis, MO).

Force apparatus

All single-molecule force measurements were conducted using a home-built AFM that employs a single axis piezoelectric translator equipped with a strain gauge (Physik Instrumente, Waldbronn, Germany) to control the absolute position of the AFM cantilever (Chen and Moy, 2002). The deflection of the cantilever was monitored optically by using an inverted optical system attached to the AFM. A focused laser spot from a fiber-coupled diode laser (Oz Optics, Nepean, ON, Canada) was reflected off the back of the cantilever onto a two-segment photodiode to monitor the cantilever's deflection. The photodiode signal was preamplified, digitized, and processed by an Apple Power Macintosh computer. The sample holder of the apparatus was designed to accept a standard 35-mm tissue culture dish. The force apparatus was suspended within a refrigerator housing to reduce both mechanical and thermal instabilities.

Attachment of live cells to the AFM cantilever

The human monocytic cell line U937 (ATCC, Manassas, VA) was maintained in RPMI 1640 medium supplemented with 10% fetal bovine serum, 1% glutamine, 50 U/mL penicillin, and 50 μg/mL streptomycin in 5% CO_2 at 37°C until needed. Individual U937 cells were attached to the AFM cantilever via concanavalin A (Con A)-mediated linkages (Benoit, 2002; Zhang et al., 2002). To prepare the Con A-functionalized cantilever, the cantilevers were soaked in acetone for 5 min, ultraviolet-irradiated for 30 min, and incubated in biotinamidocaproyl-labeled bovine serum albumin (BSA) (biotin-BSA, 0.5 mg/mL in 100 mM $NaHCO_3$, pH 8.6) overnight at 37°C. The cantilevers were then rinsed three times with PBS (10 mM PO_4^{3-}, 150 mM NaCl, pH 7.3) and incubated in streptavidin (0.5 mg/mL in phosphate-buffered saline (PBS)) for 10 min at room temperature. After the removal of unbound streptavidin, the cantilevers were incubated in biotinylated Con A (0.5 mg/mL in PBS) and then rinsed with PBS. To attach the cell to the cantilever, the tip of the Con A-functionalized cantilever was positioned above the center of a cell and lowered onto the cell for ~1 s. AFM measurements using the U937 functionalized cantilever were carried out in complete culture medium supplemented with 10 mM HEPES.

AFM measurements

The AFM force measurements were performed at room temperature (25°C) in force spectroscopy mode. The AFM force measurements consisted of an approach trace that recorded the force acting on the cantilever while the cantilever was lowered onto the sample, and a retraction trace that recorded the tip/sample interaction while the cantilever was pulled away from the sample. Measurements of unitary unbinding forces were obtained under conditions that minimized contact between the functionalized cantilever and the sample. An adhesion frequency of <30% in the force measurements ensured a >83% probability that the adhesion event was mediated by a single bond (Evans et al., 2001; Tees et al., 2001). The concentrations of proteins used in the preparation of the cantilever and substrate were adjusted to achieve adhesion frequencies of 20–30%. Measurements were acquired for loading rates between 100 pN/s and 100,000 pN/s. The change of loading rates was achieved by varying the retraction speed of the cantilever from 0.03 to 30 μm/s. Cantilevers were calibrated by equating their thermal vibrational energy to that of a one-dimensional oscillator (Hutter and Bechhoefer, 1993). The spring constants (~10 mN/m) of the calibrated cantilevers agreed with the values specified by the manufacturer.

The unbinding forces of individual adhesive interactions were derived from the jump in force after the separation of the cantilever from the sample. We acquired 50–150 unbinding forces for each histogram. For measurements obtained at fast retraction rates (>1 μm/s), the measured unbinding force was corrected for hydrodynamic drag acting on the cantilever. The determination of hydrodynamic forces was based on a method used by Tees et al. (2001). We allowed the cantilever to undergo free movement at different speeds, and the hydrodynamic force for each speed was measured. The damping coefficient of the cantilever in the experimental solution was ~2 pN-s/μm.

Dynamic force spectroscopy

Our analysis of the unbinding of the $\alpha_4\beta_1$/VCAM-1 complex employed the Bell-Evans model (Bell, 1978; Evans and Ritchie, 1997), which has been applied to studies of other ligand-receptor systems (Chen and Springer, 2001; Evans et al., 2001; Merkel et al., 1999). In the context of this model, a pulling force f distorts the energy landscape of the ligand-receptor complex, resulting in a lowering of the activation barrier(s), and consequently increases the dissociation rate constant $k(f)$ as follows:

$$k(f) = k^0 \exp[f\gamma/k_BT], \tag{1}$$

where k^0 is the dissociation rate constant in the absence of the pulling force, γ is the width of the potential barrier projected along the direction of the applied force, T is absolute temperature, and k_B is Boltzmann's constant. Under conditions of a constant loading rate r_f ($r_f = df/dt$), the probability density function for the unbinding of a complex at force f is given by (Evans and Ritchie, 1997):

$$P(f) = k^0 \exp\left\{\frac{\gamma f}{k_BT}\right\}\exp\left\{\frac{k^0 k_BT}{\gamma r_f}\left[1 - \exp\left(\frac{\gamma f}{k_BT}\right)\right]\right\}. \tag{2}$$

From Eq. 2, the most probable force f^* (i.e., the maximum of the distribution $\partial P(f)/\partial f = 0$) is

$$f^* = \frac{k_BT}{\gamma}\ln\left\{\frac{\gamma}{k^0 k_BT}\right\} + \frac{k_BT}{\gamma}\ln\{r_f\}. \tag{3}$$

Hence, Eq. 3 shows that the most probable unbinding force f^* is a linear function of the logarithm of the loading rate. Experimentally, the most probable unbinding force f^* was obtained from the mode of the unbinding force histogram. The Bell model parameters k^0 and γ were obtained from the plot of f^* versus $\ln(r_f)$.

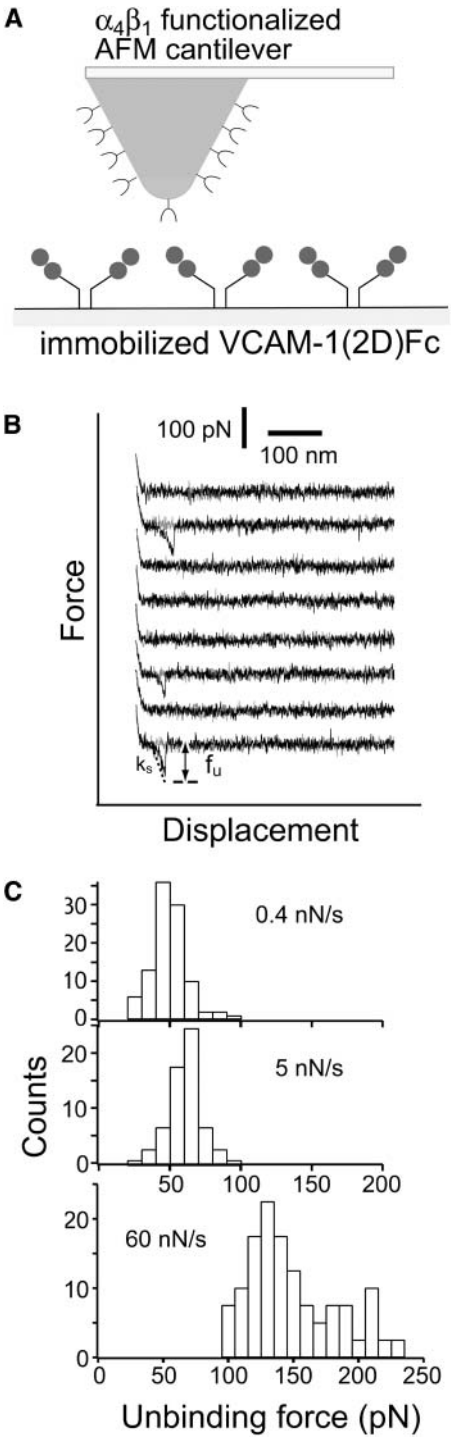

FIGURE 1 AFM force measurements of the $\alpha_4\beta_1$-Fc/VCAM-1(2D)Fc interaction. (*A*) Schematic of the experimental system. $\alpha_4\beta_1$-Fc was coupled to the AFM cantilever via a glutaraldehyde linkage (Moy et al., 1999). The cantilevers were initially silanized with 3-aminopropyltriethoxysilane to introduce an amino group on the cantilever surface. After incubation of the cantilevers with 0.1% glutaraldehyde for 30 min, $\alpha_4\beta_1$-Fc (100–200 μg/ml) was coupled to the cantilever through the glutaraldehyde linker. BSA (100 μg/mL) in Tris buffered saline (30 mM Tris, 150 mM NaCl, pH 7.5) was used to block the bare surfaces of the cantilever. VCAM-1(2D)/Fc was immobilized onto the Petri dish by passive adsorption (Wojcikiewicz et al., 2003; Zhang et al., 2002). Thirty μL of VCAM-1(2D)/Fc at 5 μg/ml in 0.1 M $NaHCO_3$ (pH 8.6) was adsorbed overnight at 4°C on the center of a 35-mm tissue culture dish (Falcon, BD Biosciences, San Jose, CA). Higher protein concentrations (20–100 μg/ml) were used in the VCAM-1 mutant experiments. Before each experiment, both the functionalized cantilever and the coated dish were blocked with BSA at 100 μg/mL. (*B*) A series of eight consecutive AFM force-displacement curves. The AFM measurements were acquired with an adhesion frequency of ~30% in Tris-buffered saline plus 2 mM of Mg^{2+}. f_u is the unbinding force of the $\alpha_4\beta_1$/VCAM-1 complex. k_s is the system spring constant and was derived from the slope of the force-displacement trace. The speed of cantilever retraction was 1300 nm/s. The force loading rate was ~5 nN/s. (*C*) Force histograms of unitary $\alpha_4\beta_1$-Fc/VCAM-1(2D)Fc unbinding forces for three different loading rates.

RESULTS

Dynamic strength of the $\alpha_4\beta_1$/VCAM-1 complex

Single-molecule AFM force measurements (Florin et al., 1994; Lee et al., 1994) were carried out to characterize the dynamic strength of the $\alpha_4\beta_1$/VCAM-1 interaction. Fig. 1 *A* illustrates our experimental system, which consisted of an AFM cantilever decorated with recombinant $\alpha_4\beta_1$-Fc and purified VCAM-1(2D)Fc immobilized on a tissue culture dish. $\alpha_4\beta_1$-Fc is a soluble form of human $\alpha_4\beta_1$, produced as a Fc chimera after fusion of the cDNAs encoding the ectodomains of each subunit to genomic DNA encoding the Fc of human γ_1 IgG (Stephens et al., 2000). Both $\alpha_4\beta_1$-Fc and native $\alpha_4\beta_1$ bind VCAM-1 with an apparent K_d of 0.2–0.3 nM (Stephens et al., 2000). VCAM-1(2D)Fc is a recombinant truncated form of VCAM-1 consisting of domains 1 and 2 of human VCAM-1 fused to the hinge of the Fc region of human IgG_1.

To assess the dynamic strength of individual $\alpha_4\beta_1$-Fc/VCAM-1(2D)Fc interactions, contact between the cantilever tip and substrate was minimized by using a small contact duration (<50 ms) and a small compression force (~100 pN). Fig. 1 *B* plots a series of eight AFM recordings of the interaction between AFM tip and substrate. Adhesion between the apposing surfaces on contact gave rise to a hysteresis between the approach (*shaded*) and retraction (*black*) traces of the measurement, as found in the second, sixth, and eighth traces of Fig. 1 *B*. The unbinding force f_u of the $\alpha_4\beta_1$-Fc/VCAM-1(2D)Fc complex is derived from the force jump that accompanies the unbinding of the complex. Sample force histograms of unbinding force obtained with different loading rates are presented in Fig. 1 *C*. These histograms show that the unbinding force increases with the loading rate of the measurements. The DFS of the $\alpha_4\beta_1$-Fc/VCAM-1(2D)Fc interaction was obtained by plotting the mode unbinding force as a function of loading rate as shown in Fig. 2 *A*. The specificity of the $\alpha_4\beta_1$-Fc/VCAM-1(2D)Fc interactions was confirmed by a reduction in the frequency of adhesion after the addition of a function-blocking antibody against VCAM-1 (e.g., AF809) or free VCAM-1(2D)Fc molecules (Fig. 2 *B*). To test whether the adsorbed VCAM-1(2D)Fc was pulled off the substrate rather than separating

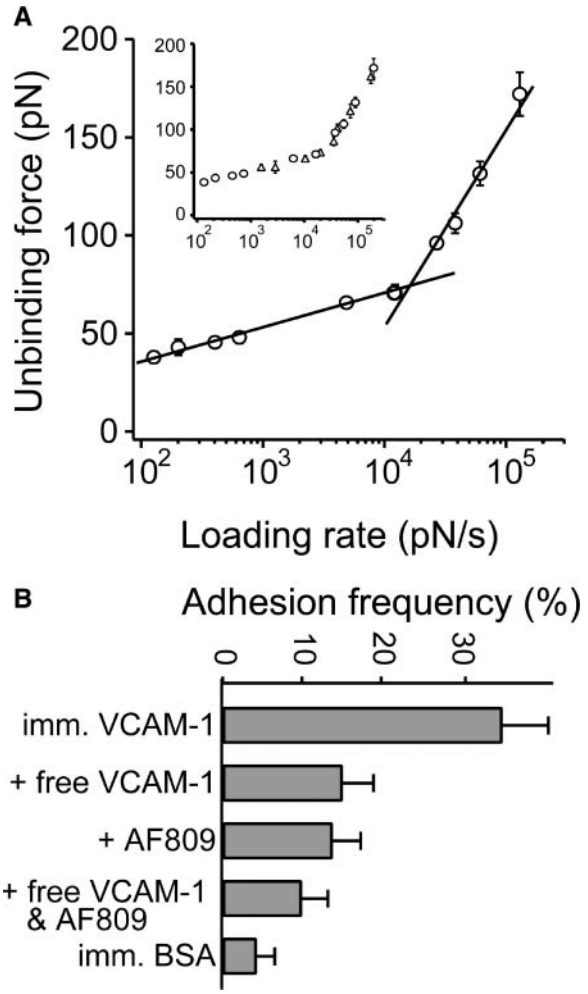

FIGURE 2 Dynamic force spectroscopy of the $\alpha_4\beta_1$-Fc/VCAM-1(2D)Fc interaction. (*A*) Dynamic force spectra of the $\alpha_4\beta_1$/VCAM-1 complexes in 2 mM Mg^{2+}. The most probable unbinding forces were obtained from the mode of the unbinding-force histogram, i.e., the tallest bin in the histogram. The best-fit curves (*solid lines*) were obtained using Eq. 3. (*Inset*) Different immobilization method of VCAM-1 (*circles*, passive adsorption; *triangles*: covalent linkage). Error bars indicate the standard error of the mean. Some error bars are within the symbol. (*B*) Adhesion frequency in AFM measurements of the $\alpha_4\beta_1$/VCAM-1 interactions under different conditions. Error bars indicate standard error of the mean. The final concentrations of AF809 (anti-VCAM-1) and free VCAM-1(2D)Fc used in the inhibition experiments were both 50 μg/mL.

from the $\alpha_4\beta_1$-Fc of the AFM tip during our measurements, we covalently coupled VCAM-1(2D)Fc to a glass coverslip (Moy et al., 1999). As shown in the insert of Fig. 2 *A*, the covalent immobilization method and the passive adsorption method yielded indistinguishable DFS, thus confirming that the measured rupture forces correspond to the unbinding of the $\alpha_4\beta_1$-Fc/VCAM-1(2D)Fc complex.

As shown in Fig. 2 *A*, $\alpha_4\beta_1$-Fc/VCAM-1(2D)Fc force spectra can be divided into two regimes within the range of loading rates accessible by our instrument. Beginning at 150 pN/s, the unbinding force increased exponentially with loading rate up to ~20,000 pN/s. Beyond this point, a faster exponential increase is clearly evident. A theoretical framework for understanding how a pulling force affects the dissociation rate of adhesion complex was proposed by Bell (1978). In this model, the dissociation potential of an adhesion complex is characterized by two parameters: k^0 is the dissociation rate constant in the absence of force and γ is the position of the transition state of the complex. Recently, Evans showed that molecular dissociation of a complex that involves overcoming more than one activation barrier may result in a DFS that reveals several exponential domains distinguishable by differences in slopes (Evans and Ritchie, 1997; Merkel et al., 1999). Our DFS of the $\alpha_4\beta_1$-Fc/VCAM-1(2D)Fc interaction is consistent with an intermolecular potential that includes two activation energy barriers. The barriers are characterized by two force-loading regimes in the DFS: slow (150–20,000 pN/s) and fast (20,000–100,000 pN/s) (Fig. 2 *A*). Fitting Eq. 3 (see Methods) to the slow and fast regimes gives the Bell model parameters (i.e., k^0 and γ) for outer and inner barriers, respectively (see Table 1). Based on this analysis, the estimated widths of the inner and outer barriers are ~1 and 5.9 Å, respectively.

Contributions of D1 of VCAM-1

Previous studies suggest that divalent cations are essential for the formation of the inner barrier of both $\alpha_5\beta_1$/fibronectin and $\alpha_L\beta_2$/ICAM-1 complexes (Li et al., 2003; Zhang et al., 2002). Likewise, the $\alpha_4\beta_1$/VCAM-1 interaction involves a Mg^{2+} ion that is chelated by the MIDAS site of the β A-domain and interacts with the Asp-40 residue in domain 1 of VCAM-1 (Wang and Springer, 1998). Hence, we postulate that the inner barrier in the $\alpha_4\beta_1$/VCAM-1 interaction is largely due to the strong ionic interaction between the chelated Mg^{2+} and the negatively charged Asp-40 residue. Indeed, the presence of 5 mM EDTA eliminated the inner activation barriers of the $\alpha_4\beta_1$/VCAM-1 complex (Fig. 3), as previously observed in the $\alpha_L\beta_2$/ICAM-1 interaction. However, this EDTA effect could be due to a direct or

TABLE 1 Bell model parameters of the $\alpha_4\beta_1$/VCAM-1 complexes

Condition	γ_1(Å)	$k_1^0(s^{-1})$	γ_2(Å)	$k_2^0(s^{-1})$
Wild-type	1.0 ± 0.1	59 ± 7	5.9 ± 0.2	0.13 ± 0.02
5 mM EDTA	—	—	3.8 ± 0.3	9.3 ± 0.4
D40A	—	—	5.9 ± 0.4	1.2 ± 0.3
D40E	2.7 ± 0.1	16 ± 2	5.5 ± 0.1	1.0 ± 0.3
Q38G	1.7 ± 0.1	65 ± 10	5.8 ± 0.2	0.46 ± 0.06
L43K	1.5 ± 0.1	60 ± 8	5.7 ± 0.1	1.7 ± 0.4
D143A	0.95 ± 0.05	72 ± 4	5.8 ± 0.1	0.85 ± 0.05

The Bell model parameters were given by fitting Eq. 3 to the acquired measurements. Linear regression was done using IgorPro software. The indices 1 and 2 in the subscript of the Bell model parameters refer to the inner and outer barriers of the complex, respectively. The goodness of fit was determined by R^2, the square of the correlation coefficient. An R^2 of 0.95 was chosen as the cutoff point to determine the transition point between the slow and the fast loading regimes.

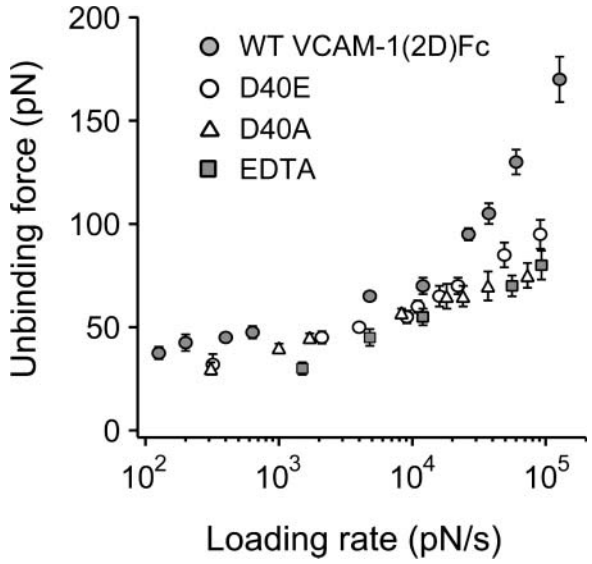

FIGURE 3 Molecular determinants of the inner activation barriers of the $\alpha_4\beta_1$-Fc/VCAM-1(2D)Fc complex. Effects of EDTA and mutations in the Asp-40 residue of VCAM-1. Error bars indicate standard error of the mean. When not visible, error bars are within the symbol.

indirect contribution of the divalent cation to the formation of the inner activation barrier since it is conceivable that the β A-domain is not folded properly in the absence of Mg^{2+}. To further investigate the nature of divalent cation action, we investigated the interaction between $\alpha_4\beta_1$ and two VCAM-1 mutants that have a single amino acid substitution at the Asp-40 residue. Mutating the Asp-40 residue of VCAM-1 to the neutral residue, alanine (D40A), suppressed the unbinding forces of the $\alpha_4\beta_1$/VCAM-1 interaction, most noticeably in the high loading regime of the DFS (Fig. 3). However, when Asp-40 is substituted by the negatively charged residue glutamate (D40E), the fast loading regime is still distinguishable from the slow loading regime, indicating that the inner activation barrier is suppressed, but not eliminated.

A more detailed analysis of the measurements on the VCAM-1 mutants was achieved by fitting the Bell model to the acquired DFS. Table 1 summarizes the Bell model parameters for the different $\alpha_4\beta_1$/VCAM-1 (mutants) complexes. Both EDTA treatment and the D40A mutation completely eliminated the inner activation barrier, whereas the D40E mutation widened the inner barrier from 1 Å to 2.7 Å. As discussed below, the consequence of this widening of the inner barrier is that the dissociation rate of the complex becomes more responsive to changes in pulling force in the high force regime. The effects of EDTA treatment and both D40 mutations on the outer activation barrier were similar, resulting in a suppression of the outer barrier as indicated by the 10-fold increase in the dissociation rate for the outer barrier. Taken together, these data demonstrate that the inner barrier of the $\alpha_4\beta_1$-Fc/VCAM-1(2D)Fc complex requires both the divalent cation Mg^{2+} and the Asp-40 residue of VCAM-1. The absence of this ionic interaction also destabilized the outer activation barrier.

In addition to Asp-40, we also explored the role of other residues in the C-D loop of the first domain of VCAM-1, including Gln-38 and Leu-43. Fig. 4 *A* shows that the two C-D loop mutants Q38G and L43K yielded similar DFS. Compared with the wild-type VCAM-1, these mutants have smaller unbinding forces in both the slow and fast loading regimes. The Bell model parameters of these two mutants reveal that the reduced unbinding forces are largely due to a widening in the inner barrier and a suppression in the height of the outer barrier (i.e., larger k_2^0). Differences in the dynamic strength of our C-D loop mutants (i.e., D40A, D40E, Q38G, and L43K) appears to be due to a difference in the width of the inner barrier (i.e., γ_1).

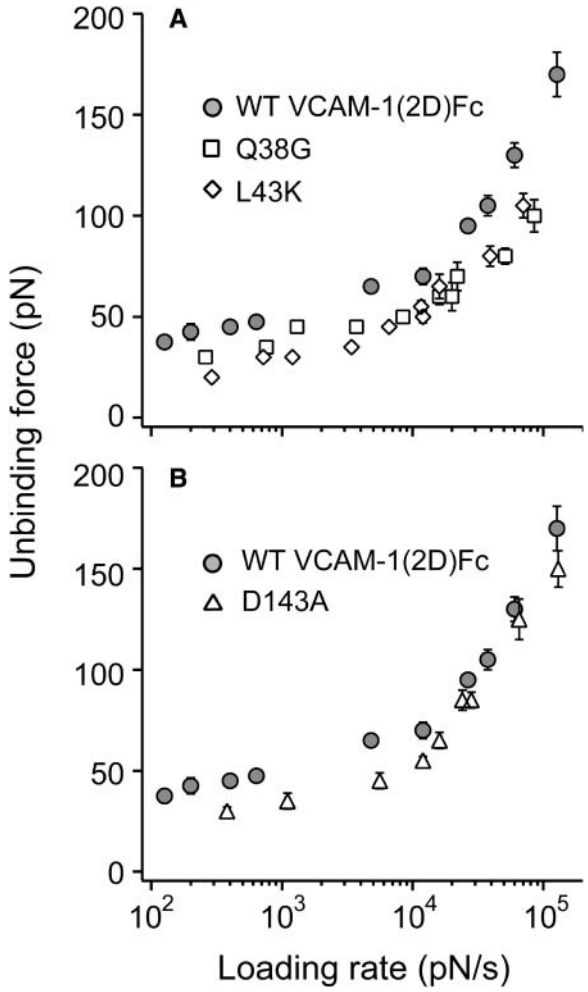

FIGURE 4 Molecular determinants of the outer activation barriers of the $\alpha_4\beta_1$-Fc/VCAM-1(2D)Fc complex. (*A*) Effect of mutations in the C-D loop of VCAM-1. (*B*) Effect of mutations in the D2 of VCAM-1. Error bars indicate standard error of the mean. When not visible, error bars are within the symbol.

Contributions of D2 of VCAM-1

Newham et al. have shown that certain mutations in the D2 of VCAM-1 (i.e., D143A, S148A, and E150A) also affected binding to $\alpha_4\beta_1$ (Newham et al., 1997). These mutations were previously identified as having a marked effect on the $\alpha_4\beta_1$ binding, though it is not known how these mutations modified $\alpha_4\beta_1$ binding. It has been proposed that the interaction between D2 of VCAM-1 and $\alpha_4\beta_1$ is analogous to the interaction between $\alpha_5\beta_1$ and the synergy site in FNIII9 of fibronectin. We have previously shown that the synergy site of FNIII9 helps stabilize the outer activation barrier of the $\alpha_5\beta_1$/fibronectin interaction (Li et al., 2003). To test if D2 of VCAM-1 has a similar role, we acquired the DFS of $\alpha_4\beta_1$ interacting with one of the D2 mutants (i.e., D143A) and found that the mutation suppressed the unbinding force in the slow loading regime, but had no effect on forces in the fast loading regime (Fig. 4 *B*). A comparison of the Bell model parameters obtained using wild-type VCAM-1 and its D143A mutant reveals that the only difference between the wild-type and mutant interactions is a reduction in the height of the outer activation barrier of mutant complex. These results suggest that D2 of VCAM-1 helps stabilize the activation energy of the outer barrier of the $\alpha_4\beta_1$/VCAM-1 complex.

Dynamic strength of the native $\alpha_4\beta_1$/VCAM-1 complex in live cells

An important attribute of integrins is their ability to modulate the adhesive states of cells (Diamond and Springer, 1994; Dustin and Springer, 1989; Humphries et al., 2003; Shimaoka et al., 2002). In resting leukocytes, $\alpha_4\beta_1$ is expressed in an inactive, nonadhesive state that binds VCAM-1 with low affinity. Upon activation, the leukocyte expresses an activated form of $\alpha_4\beta_1$ and becomes adherent to the endothelium. The induction of high-affinity $\alpha_4\beta_1$ is presumably due to the unclasping and separation of the integrin α and β cytoplasmic tails, leading to changes in the conformation and/or orientation of the N-terminal domains of both the α and β subunits (Carman and Springer, 2003).

To determine if the VCAM-1 binding properties of our recombinant $\alpha_4\beta_1$-Fc resembles that of native $\alpha_4\beta_1$, we measured the DFS of $\alpha_4\beta_1$/VCAM-1(2D) interaction on live U937 cells (Fig. 5 *A*). U937 is a monocytic cell line that has been used in previous studies of $\alpha_4\beta_1$ mediated adhesion (Chigaev et al., 2003). The expression of $\alpha_4\beta_1$ on U937 cells was confirmed by flow cytometry (data not shown). The high-affinity form of $\alpha_4\beta_1$ was induced by activation antibody TS2/16, bypassing the requirements of inside-out signal from the cells (Alon et al., 1995; Chen et al., 1999; Li et al., 2003). As shown in Fig. 5 *B*, the DFS of native $\alpha_4\beta_1$/VCAM-1 complexes also displayed two loading regimes, similar to the results obtained with recombinant $\alpha_4\beta_1$-Fc. After activation by TS2/16, the unbinding forces of the native $\alpha_4\beta_1$/VCAM-1(2D) complex were elevated over the

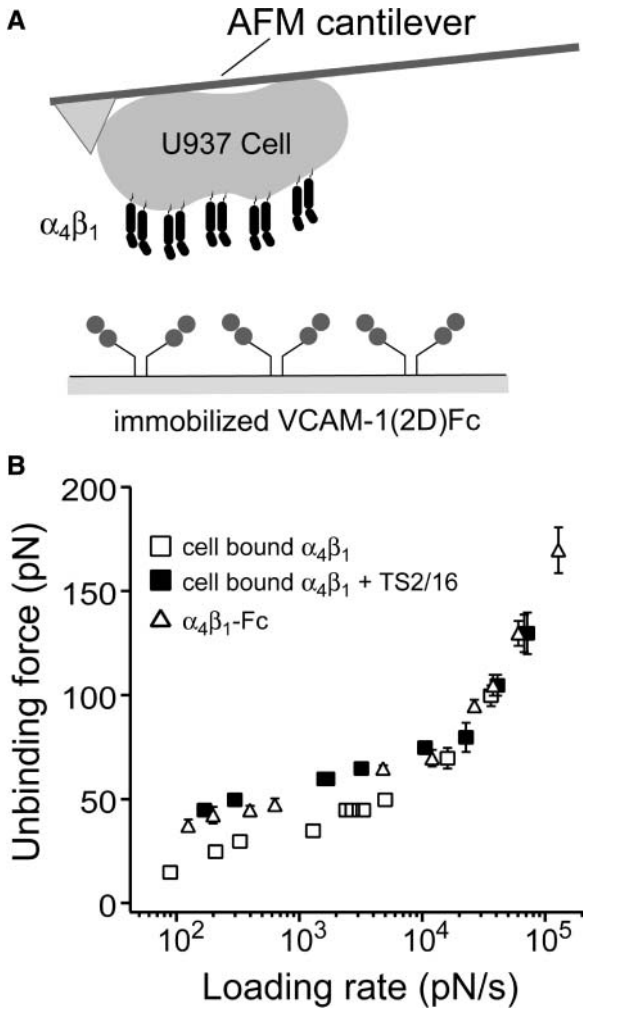

FIGURE 5 DFS of $\alpha_4\beta_1$/VCAM-1 interaction on live U937 cells. (*A*) Schematic diagram of the AFM experiments. (*B*) DFS of the high- and the low-affinity $\alpha_4\beta_1$/VCAM-1 interaction. The AFM measurements were acquired under single-molecule conditions. High-affinity $\alpha_4\beta_1$ was induced by TS2/16. Specificity of the measurement has been confirmed by antibody blocking experiments. Error bars indicate standard error of the mean. When not visible, error bars are within the symbol.

range of loading rates between 100 and 20,000 pN/s, but did not significantly change at loading rates >20,000 pN/s. Fig. 5 *B* also reveals that the DFS of $\alpha_4\beta_1$-Fc/VCAM-1(2D)Fc interaction is nearly identical to that of the high-affinity native $\alpha_4\beta_1$/VCAM-1(2D)Fc interaction. Moreover, the presence of the TS2/16 antibody did not change the DFS of the $\alpha_4\beta_1$-Fc/VCAM-1(2D)Fc interaction. Hence, we conclude that $\alpha_4\beta_1$-Fc is locked in a conformational state that resembles the high-affinity conformer of native $\alpha_4\beta_1$.

Table 2 lists the Bell model parameters of the native $\alpha_4\beta_1$/VCAM-1(2D) interaction. The dissociation rates of the outer barrier for low- and high-affinity $\alpha_4\beta_1$/VCAM-1 complexes were 1.4/s and 0.035/s, respectively, reflecting a difference in the energy of the outer barrier. However, no significant difference ($P > 0.05$) was found in dissociation rates (~100/s) for the inner barrier of both affinity states. Thus, DFS of the

TABLE 2 Bell model parameters of the low and high affinity $\alpha_4\beta_1$/VCAM-1 complexes

Ligand-receptor pair	Conditions	γ_1(Å)	$k_1^0(s^{-1})$	γ_2(Å)	$k_2^0(s^{-1})$
Memb. $\alpha_4\beta_1$/VCAM-1	Resting	0.93 ± 0.06	63 ± 10	5.2 ± 0.3	1.1 ± 0.2
	TS2/16	0.99 ± 0.03	75 ± 5	6.2 ± 0.6	0.04 ± 0.02
$\alpha_4\beta_1$-Fc/VCAM-1	Mg^{2+}	1.0 ± 0.1	59 ± 7	5.9 ± 0.2	0.13 ± 0.02

The Bell model parameters were given by fitting Eq. 3 to the acquired measurements. Linear regression was done using IgorPro software. The indices 1 and 2 in the subscript of the Bell model parameters refer to the inner and outer barriers of the complex, respectively. The goodness of fit was determined by R^2, the square of the correlation coefficient. An R^2 of 0.95 was chosen as the cutoff point to determine the transition point between the slow and the fast loading regimes.

native $\alpha_4\beta_1$/VCAM-1 interaction shows that induction of high-affinity $\alpha_4\beta_1$ by TS2/16 elevates the energy potential of their outer activation barriers, but has minimal effect on the inner barriers. It should be noted that activation of other integrins including $\alpha_L\beta_2$ and $\alpha_5\beta_1$ also manifested in an elevation of the outer activation barrier. Together, these observations suggest that integrin activation, in general, involves changes in height of the outer activation barrier and hence the K_d of the complex.

DISCUSSION

Using the k^0 and γ values from Table 1, we were able to estimate the energy landscape of the $\alpha_4\beta_1$/VCAM-1 complex. As summarized in Fig. 6 *A*, the dissociation of the $\alpha_4\beta_1$/VCAM-1 bond involves overcoming two activation barriers: a steep inner barrier and a more elevated outer barrier. The position of the transition states was estimated by the Bell model parameter γ. Estimates of the energy difference between the transition states were calculated as $\Delta G_{12} = -k_BT\ln(k_1^0/k_2^0)$, where k_1^0 and k_2^0 are the dissociation rate constants of transition states 1 and 2, respectively. The energy level of the bound complex was arbitrarily chosen. Mutation at the Asp-40 residue of VCAM-1, i.e., D40A, eliminated the inner barrier and lowered the outer barrier by 2.3 k_BT. The C-D loop mutant L43K lowered the outer barrier by 3 k_BT and widened the inner barrier. However, D143A, a mutation in the D2 of VCAM-1, did not alter the inner barrier, but lowered the outer barrier by 2.3 k_BT.

The effects of a pulling force on the dissociation rate constant of a molecular complex with two activation barriers is given by

$$k_{off} = 1/\{k_1^{0^{-1}}\exp[-f\gamma_1/k_BT] + k_2^{0^{-1}}\exp[-f\gamma_2/k_BT]\}, \quad (4)$$

where the subscripts 1 and 2 refer to inner and outer activation energy barriers, respectively (Evans et al., 2001). The force-dependent dissociation rate of the $\alpha_4\beta_1$/VCAM-1 (mutant) complexes computed using Eq. 4 and the derived Bell model parameters are shown in Fig. 6, *B* and *C*. Under pulling forces $<\sim$50 pN, the dissociation rate is highly sensitive to pulling forces and is governed principally by the properties of the outer barrier (i.e., γ_2 and k_2^0). At stronger forces, the dissociation rate is governed by the inner barrier and is less responsive to changes in pulling force. In the absence of the inner barrier, as seen when the Asp-40 residue is mutated to Ala, the dissociation rate of the complex continues to increase exponentially with pulling force. When Asp-40 is mutated to Glu (D40E), the inner barrier remains, though suppressed. As a result, the D40E mutant is expected to show some force resistance above 50 pN. In contrast, mutations that suppress just the outer barrier, as in the D143A mutant, have a greater effect on the dissociation rate of the complex at pulling forces $<$50 pN.

It is worthwhile to compare the dynamic response of the $\alpha_4\beta_1$/VCAM-1 complex with other leukocyte adhesion complexes involved in the extravasation and to relate the intrinsic biophysical properties of the adhesion complexes to their function at the cellular level. The process of leukocyte extravasation involves multiple stages: rolling, cell activation, firm adhesion, and, finally, transmigration. Each stage engages a different set of adhesion molecules (Springer, 1994). Leukocyte rolling is mediated mainly by the selectin family molecules, whereas firm adhesion is mediated by the activated integrins and their adhesive ligands (Kubes, 2002). Specifically, the L-selectin/ligand and $\alpha_L\beta_2$/ICAM-1 interactions are known to mediate leukocyte rolling and firm adhesion, respectively (Lawrence and Springer, 1991), while the $\alpha_4\beta_1$/VCAM-1 interaction could mediate both leukocyte rolling and firm adhesion (Alon et al., 1995; Kubes, 2002). Recently, the mechanical properties of the L-selectin/sLeX complex and the $\alpha_L\beta_2$/ICAM-1 complex were characterized by single-molecule DFS (Evans et al., 2001; Zhang et al., 2002), thus allowing for a comparison of the key molecular components of leukocyte extravasation. An examination of kinetic profiles of the three complexes revealed that the force-dependent dissociation rate of the L-selectin/sLeX complex is faster and more sensitive to a pulling force than the $\alpha_L\beta_2$/ICAM-1 complex (Fig. 7), suggesting that the L-selectin/sLeX interaction is better suited for cell rolling because, in this capacity the adhesion complex should be transient and need to dissociate readily during cell rolling (Orsello et al., 2001). Not surprisingly, the more force-resistant $\alpha_L\beta_2$/ICAM-1 complex is better suited for facilitating firm adhesion. The kinetic profile of the $\alpha_4\beta_1$/VCAM-1 complex provides a likely explanation of how this complex is able to

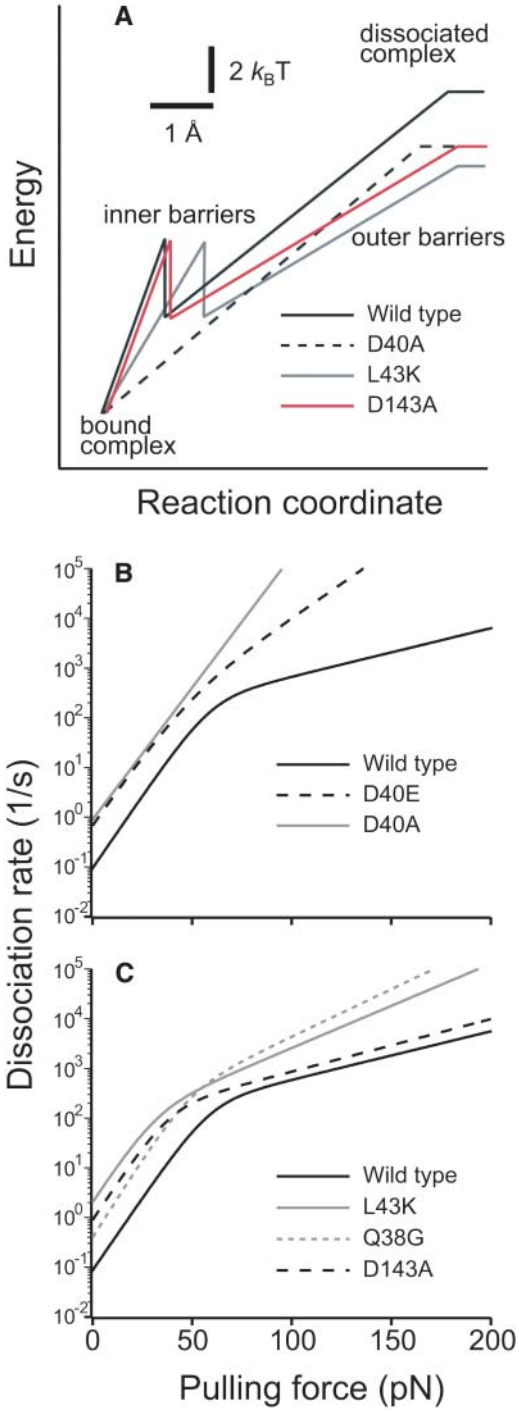

FIGURE 6 Energy and kinetic profiles of the $\alpha_4\beta_1$/VCAM-1 (mutant) complexes. (*A*) Dissociation potential of the $\alpha_4\beta_1$/VCAM-1 interaction. The forced dissociation of the $\alpha_4\beta_1$/VCAM-1 bond involves overcoming two activation energy barriers. Positions and energies of the transition states of the $\alpha_4\beta_1$/wild-type VCAM-1, and $\alpha_4\beta_1$/VCAM-1 mutant complexes are shown. (*B* and *C*) Kinetic profiles of the $\alpha_4\beta_1$/VCAM-1 mutant complexes. (*B*) Effect of mutations in the Asp-40 residue. (*C*) Effect of mutations at the C-D loop of D1 or at the Asp-143 residue of D2 of VCAM-1. The force-dependent dissociation rate of the complex was given by Eq. 4.

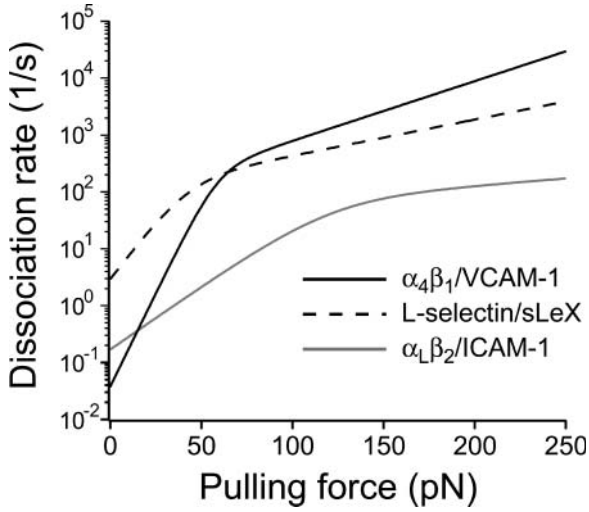

FIGURE 7 Kinetic profiles for the high-affinity $\alpha_4\beta_1$/VCAM-1, L-selectin/sLeX and high-affinity $\alpha_L\beta_2$/ICAM-1 interactions. The force-dependent dissociation rate of the complex was given by Eq. 4. Bell model parameters for the L-selectin/sLeX and high-affinity $\alpha_L\beta_2$/ICAM-1 complexes were obtained from Evans et al. (2001) and Zhang et al. (2002), respectively.

mediate both cell rolling and firm adhesion. As revealed in Fig. 7, the dissociation kinetics of $\alpha_4\beta_1$/VCAM-1 bond resembles more the kinetic profile of the L-selectin/sLeX complex at pulling force $>\sim$50pN. However, at weak pulling forces, the off rate of the $\alpha_4\beta_1$/VCAM-1 bond is comparable to that of the $\alpha_L\beta_2$/ICAM-1 complex. Previous flow-chamber experiments revealed that the shear force exerted on a single selectin bond ranged between 50 and 250 pN (Chen and Springer, 2001; Smith et al., 1999). In this force region, the mechanical properties of the $\alpha_4\beta_1$/VCAM-1 bond resemble the selectin bond and are suitable for rolling. However, when the leukocyte is activated and more integrin complexes are formed, the pulling force shared by individual $\alpha_4\beta_1$/VCAM-1 complex may be $<$50 pN. Within this force range, the off rate of the $\alpha_4\beta_1$/VCAM-1 complex is similar to the $\alpha_L\beta_2$/ICAM-1 bond and thus capable of facilitating firm adhesion.

In summary, DFS of the $\alpha_4\beta_1$/VCAM-1 complexes reveal that the dissociation of this complex involves overcoming at least two activation barriers. As a result of the steep inner barrier, the complex is less sensitive to large pulling forces. Using the VCAM-1 mutants, we found that the Asp-40 residue directly forms the inner activation barrier by interacting with the chelated Mg^{2+} ion, and that the C-D loop participates in the generation of the outer barrier and helps maintain the inner barrier. The kinetic profile of the $\alpha_4\beta_1$/VCAM-1 complex shows similarity to the L-selectin/sLeX complex in strong pulling forces, but its off rates resemble the $\alpha_L\beta_2$/ICAM-1 complex in lower pulling forces. This special kinetic profile may reflect a biophysical basis that permits a dual physiological function (i.e., cell rolling and firm adhesion) of the $\alpha_4\beta_1$/VCAM-1 interaction.

This work was supported by grants from the National Institutes of Health (GM55611) and the Wellcome Trust. X.Z. was supported by a predoctoral fellowship (0215139B) from the American Heart Association.

REFERENCES

Alon, R., P. D. Kassner, M. W. Carr, E. B. Finger, M. E. Hemler, and T. A. Springer. 1995. The integrin VLA-4 supports tethering and rolling in flow on VCAM-1. *J. Cell Biol.* 128:1243–1253.

Bell, G. I. 1978. Models for the specific adhesion of cells to cells. *Science.* 200:618–627.

Benoit, M. 2002. Cell adhesion measured by force spectroscopy on living cells. *Methods Cell Biol.* 68:91–114.

Binnig, G., C. F. Quate, and C. Gerber. 1986. Atomic force microscope. *Phys. Rev. Lett.* 56:930–933.

Carman, C. V., and T. A. Springer. 2003. Integrin avidity regulation: are changes in affinity and conformation underemphasized? *Curr. Opin. Cell Biol.* 15:547–556.

Chen, A., and V. T. Moy. 2002. Single molecule force measurements. *Methods Cell Biol.* 68:301–309.

Chen, L. L., A. Whitty, R. R. Lobb, S. P. Adams, and R. B. Pepinsky. 1999. Multiple activation states of integrin alpha4beta1 detected through their different affinities for a small molecule ligand. *J. Biol. Chem.* 274:13167–13175.

Chen, S., and T. A. Springer. 2001. Selectin receptor-ligand bonds: formation limited by shear rate and dissociation governed by the Bell model. *Proc. Natl. Acad. Sci. USA.* 98:950–955.

Chigaev, A., G. Zwartz, S. W. Graves, D. C. Dwyer, H. Tsuji, T. D. Foutz, B. S. Edwards, E. R. Prossnitz, R. S. Larson, and L. A. Sklar. 2003. Alpha4beta1 integrin affinity changes govern cell adhesion. *J. Biol. Chem.* 278:38174–38182.

Diamond, M. S., and T. A. Springer. 1994. The dynamic regulation of integrin adhesiveness. *Curr. Biol.* 4:506–517.

Dustin, M. L., and T. A. Springer. 1989. T-cell receptor cross-linking transiently stimulates adhesiveness through LFA-1. *Nature.* 341:619–624.

Evans, E., A. Leung, D. Hammer, and S. Simon. 2001. Chemically distinct transition states govern rapid dissociation of single L-selectin bonds under force. *Proc. Natl. Acad. Sci. USA.* 98:3784–3789.

Evans, E., and K. Ritchie. 1997. Dynamic strength of molecular adhesion bonds. *Biophys. J.* 72:1541–1555.

Florin, E. L., V. T. Moy, and H. E. Gaub. 1994. Adhesion forces between individual ligand-receptor pairs. *Science.* 264:415–417.

Hemler, M. E., C. Huang, and L. Schwarz. 1987. The VLA protein family. Characterization of five distinct cell surface heterodimers each with a common 130,000 molecular weight beta subunit. *J. Biol. Chem.* 262: 3300–3309.

Hörber, J. K., and M. J. Miles. 2003. Scanning probe evolution in biology. *Science.* 302:1002–1005.

Humphries, M. J., P. A. McEwan, S. J. Barton, P. A. Buckley, J. Bella, and A. Paul Mould. 2003. Integrin structure: heady advances in ligand binding, but activation still makes the knees wobble. *Trends Biochem. Sci.* 28:313–320.

Hutter, J. L., and J. Bechhoefer. 1993. Calibration of atomic-force microscope tips. *Rev. Sci. Instrum.* 64:1868–1873.

Kubes, P. 2002. The complexities of leukocyte recruitment. *Semin. Immunol.* 14:65–72.

Kunkel, T. A., J. D. Roberts, and R. A. Zakour. 1987. Rapid and efficient site-specific mutagenesis without phenotypic selection. *Methods Enzymol.* 154:367–382.

Lawrence, M. B., and T. A. Springer. 1991. Leukocytes roll on a selectin at physiologic flow rates: distinction from and prerequisite for adhesion through integrins. *Cell.* 65:859–873.

Lee, G. U., D. A. Kidwell, and R. J. Colton. 1994. Sensing discrete streptavidin-biotin interactions with AFM. *Langmuir.* 10:354–361.

Li, F., S. D. Redick, H. P. Erickson, and V. T. Moy. 2003. Force measurements of the $\alpha 5\beta 1$ integrin-fibronectin interaction. *Biophys. J.* 84:1252–1262.

Merkel, R., P. Nassoy, A. Leung, K. Ritchie, and E. Evans. 1999. Energy landscapes of receptor-ligand bonds explored with dynamic force spectroscopy. *Nature.* 397:50–53.

Moy, V. T., E. L. Florin, and H. E. Gaub. 1994. Intermolecular forces and energies between ligands and receptors. *Science.* 266:257–259.

Moy, V. T., Y. Jiao, T. Hillmann, H. Lehmann, and T. Sano. 1999. Adhesion energy of receptor-mediated interaction measured by elastic deformation. *Biophys. J.* 76:1632–1638.

Newham, P., S. E. Craig, G. N. Seddon, N. R. Schofield, A. Rees, R. M. Edwards, E. Y. Jones, and M. J. Humphries. 1997. Alpha4 integrin binding interfaces on VCAM-1 and MAdCAM-1. Integrin binding footprints identify accessory binding sites that play a role in integrin specificity. *J. Biol. Chem.* 272:19429–19440.

Orsello, C. E., D. A. Lauffenburger, and D. A. Hammer. 2001. Molecular properties in cell adhesion: a physical and engineering perspective. *Trends Biotechnol.* 19:310–316.

Osborn, L., C. Vassallo, B. G. Browning, R. Tizard, D. O. Haskard, C. D. Benjamin, I. Dougas, and T. Kirchhausen. 1994. Arrangement of domains, and amino acid residues required for binding of vascular cell adhesion molecule-1 to its counter-receptor VLA-4 (alpha 4 beta 1). *J. Cell Biol.* 124:601–608.

Radmacher, M., R. W. Tillamnn, M. Fritz, and H. E. Gaub. 1992. From molecules to cells: imaging soft samples with the atomic force microscope. *Science.* 257:1900–1905.

Shimaoka, M., J. Takagi, and T. A. Springer. 2002. Conformational regulation of integrin structure and function. *Annu. Rev. Biophys. Biomol. Struct.* 31:485–516.

Smith, M. J., E. L. Berg, and M. B. Lawrence. 1999. A direct comparison of selectin-mediated transient, adhesive events using high temporal resolution. *Biophys. J.* 77:3371–3383.

Springer, T. A. 1990. Adhesion receptors of the immune system. *Nature.* 346:425–434.

Springer, T. A. 1994. Traffic signals for lymphocyte recirculation and leukocyte emigration: the multistep paradigm. *Cell.* 76:301–314.

Stephens, P. E., S. Ortlepp, V. C. Perkins, M. K. Robinson, and H. Kirby. 2000. Expression of a soluble functional form of the integrin alpha4beta1 in mammalian cells. *Cell Adhes. Commun.* 7:377–390.

Tees, D. F., R. E. Waugh, and D. A. Hammer. 2001. A microcantilever device to assess the effect of force on the lifetime of selectin-carbohydrate bonds. *Biophys. J.* 80:668–682.

Vonderheide, R. H., T. F. Tedder, T. A. Springer, and D. E. Staunton. 1994. Residues within a conserved amino acid motif of domains 1 and 4 of VCAM-1 are required for binding to VLA-4. *J. Cell Biol.* 125:215–222.

Wang, J., and T. A. Springer. 1998. Structural specializations of immunoglobulin superfamily members for adhesion to integrins and viruses. *Immunol. Rev.* 163:197–215.

Wojcikiewicz, E. P., X. Zhang, A. Chen, and V. T. Moy. 2003. Contributions of molecular binding events and cellular compliance to the modulation of leukocyte adhesion. *J. Cell Sci.* 116:2531–2539.

Zhang, X., E. Wojcikiewicz, and V. T. Moy. 2002. Force spectroscopy of the leukocyte function-associated antigen- 1/intercellular adhesion molecule-1 interaction. *Biophys. J.* 83:2270–2279.